The Binary System Tetradecanedioic Acid–Hexadecanedioic Acid: Polymorphism of the Components and Experimental Phase Diagram

by **Lourdes Ventolà***[a]), **Valerie Metivaud**[a]), **Laura Bayés**[a]), **Raül Benages**[a]), **Miquel Ángel Cuevas-Diarte**[a]), **Teresa Calvet**[a]), and **Denise Mondieig**[b])

[a]) Departament de Cristallografia, Mineralogia i Dipòsits Minerals, Facultat de Geologia, Universitat de Barcelona, Martí i Franquès s/n, E-08028 Barcelona
(phone: +34 934021350; fax: +34-934021340; e-mail: lourdes_ventola@yahoo.com)
[b]) Centre de Physique Moléculaire Optique et Hertzienne, UMR 5798 au CNRS Université Bordeaux I, Cours de la Libération 351, F-33405 Talence Cedex

Complementary techniques had to be applied to investigate the binary system tetradecanedioic acid ($C_{14}H_{26}O_4$)–hexadecanedioic acid ($C_{16}H_{30}O_4$), because all the forms observed have the same space group ($P2_1/c$; $Z=2$). We studied the polymorphism of the two single compounds and of their mixtures by X-ray powder diffraction, differential-scanning calorimetry (DSC), infrared spectroscopy (IR), scanning electron microscopy (SEM), and thermo-optical microscopy (TOM). The two diacids were found to be isopolymorphic. At low temperature, they crystallize in the same ordered *C*-form, and, on heating, adopt the ordered C_h-form, 1° below their melting point. In contrast to similar compounds (unbranched alkanes, alkanols, and fatty acids), the solid–solid and solid–liquid phase-transition temperatures decrease with increasing chain length. At low temperature, a new monoclinic form, C_i, appears as a result of the disorder of composition in the mixed samples. There are two [$C+C_i$]-type solid–solid domains. On heating, the solid domains are related to solid–liquid domains by a peritectic invariant for compositions rich in $C_{14}H_{26}O_4$, and by a eutectic invariant for compositions rich in $C_{16}H_{30}O_4$. At higher temperature, there appears a second peritectic invariant for compositions rich in $C_{14}H_{26}O_4$, together with a metatectic invariant for compositions rich in $C_{16}H_{30}O_4$. All the solid forms observed in this binary system are isostructural. Nevertheless, the equilibrium between them is complex near the melting point, and their miscibility in the solid state is reduced.

Introduction. – Dicarboxylic acids of the type HOOC–$(CH_2)_n$–COOH are straight-chain molecules with carboxylic groups at both ends. They form a layered structure in the solid state, as do most polymorphic phases of long-chain compounds, such as unbranched alkanes, alkanols, and fatty acids [1–6]. Owing to the presence of the COOH groups at both ends, the density of H-bonds is significantly greater in dicarboxylic acids than in fatty acids. As a consequence, their melting points are higher than those of analogous fatty acids. For example, tetradecanoic acid melts at 327.5 K, and tetradecanedioic acid melts at 398.9 K [1].

The four polymorphic forms *B*, *C*, *E* ($P2_1/c$), and *A* ($P\bar{1}$) have been described for both unbranched fatty and dicarboxylic acids [7–15]. The hydrocarbon chains adopt the all-*trans*-conformation in forms *A*, *C*, and *E*, but the *B*-form has a gauche conformation in the vicinity of the COOH group [7][9]. There is another form, called A_{super}, which has an unusual conformation in which the COOH group rotates about the C(1)–

C(2) bond. This structure can be rationalized by considering the O–O distance to an adjacent molecule [9].

We have performed a structural and energetic study of tetradecanedioic acid ($C_{14}H_{26}O_4$) and of hexadecanedioic acid ($C_{16}H_{30}O_4$), both as single compounds and as binary mixtures, to establish their experimental phase diagram. We followed a complementary approach, including X-ray powder diffraction, differential-scanning calorimetry (DSC), infrared spectroscopy (IR), scanning electron microscopy (SEM), and thermo-optical microscopy (TOM). To our knowledge, this is the first detailed study of polymorphism in long-chain dicarboxylic acids.

This research was performed by the REALM (*Réseau Européen sur les Alliages Moléculaires*) network, which is dedicated to the preparation, structural and thermodynamic characterization, modeling, and application of molecular alloys for energy storage and thermal protection [18][19].

Experimental. – *General.* The two dicarboxylic acids, $C_{14}H_{26}O_4$ and $C_{16}H_{30}O_4$, were purchased from *Fluka*, and were used without further purification. Their purity was corroborated by gas chromatography (GC) to be $\geq$99.5%. Mixed samples were obtained by 'melting quenching'. The components were weighed in the desired proportions, melted, and mixed to a homogeneous solution, and then quenched in liquid N_2.

Differential-Scanning Calorimetry (DSC). Calorimetric data were obtained with a *Perkin Elmer DSC-7* apparatus, with 3.9–4.1 mg of diacid at a scan rate of 2 K min^{-1}; six independent measurements were made for each sample ($n=6$). The instrument was calibrated by reference to the enthalpy and m.p. of indium and decane standards. The random part of the uncertainties was estimated with *Student*'s method, with a 95% threshold of reliability. The characteristic temp. was determined from the DSC curves by the shape-factor method [20]. Enthalpy effects were evaluated by integration of the DSC signals.

X-Ray Powder Diffraction. Diffraction data were recorded on *Panalytical* and *Siemens D-500* diffractometers. Spectra were recorded on the *Panalytical* diffractometer at r.t. to improve resolution and minimize orientation effects. The diffractometer was operated in the transmission mode using CuK_α radiation, with a double Mb crystal as the primary monochromator, and the sample was mounted on a sealed capillary (0.5-mm diameter) perpendicular to the X-ray radiation beam. The temp. was measured with the *Siemens D-500* diffractometer applying *Bragg–Brentano* geometry, CuK_α radiation, and a secondary monochromator. The data were collected with an *Anton PAAR TTK* system, with a heating rate of 0.02 K s^{-1} and an equilibration time of 5 min. Samples were heated from 298 K to the melting point. The patterns were scanned with a step size of 0.025° and a step time of 5 s; the 2θ range was 1.6–60°. In both cases, the cell parameters were refined with the *Pawley* profile-fitting procedure [21] of the Materials Studio software [22].

Infrared Spectroscopy. IR Spectra of finely powdered samples were recorded on a *Bomem DA3 FTIR* spectrometer at r.t. using a diffuse reflection accessory (DRIFT) in the region 450–4000 cm^{-1} at a resolution of 4 cm^{-1}. All IR measurements were run in the vacuum mode with an *MCT* wide-range detector; the beam splitter was KBr, and the source was a glow bar. Each spectrum was obtained by averaging 100 scans.

Scanning Electron Microscopy (SEM). SEM Analyses were performed at r.t. on a *Hitachi S-4100* field-emission apparatus. The polycrystalline samples were mounted on a support platform (12-mm diameter) with a conductor adhesive (*Agar Scientific*), and fixed with a thin carbon layer (*ca.* 20 nm).

Thermo-Optical Microscopy (TOM). TOM Images were obtained on a *Linkam THMSG-600* stage mounted to a *Carl Zeiss* microscope. The sample was placed on a 7-mm quartz-cover slip, and encased within a pure Ag lid so that it was heated from all sides, ensuring a uniform temp.

Results and Discussion. – 1. *Single Dicarboxylic Acids.* 1.1 *Calorimetric Measurements.* On heating, each of the two title compounds showed a single peak, with a light inflection, suggesting the presence of a solid–solid transition overlapping the solid–liquid phenomena (*Fig. 1*, *a* and *1*, *b*). The analysis at slow speed (0.2 K/min) corroborated these two transitions, making them more evident. However, it was impossible to define a clear separation between them (*Fig. 1*, *c*). On cooling (*Fig. 1*, *d* and *1*, *e*), the solid–solid and solid–liquid transitions were more evident, especially for $C_{14}H_{26}O_4$, although we were still unable to establish a clear separation. In both compounds, the two transitions were separated by a temperature gap of less than 1 K. Even when using modulated DSC, it was impossible to separate them, as the low-energy solid–solid transition was masked by the high-energy solid–liquid transition. The transition temperatures and enthalpies are listed in *Table 1*.

Table 1. *Phase-Transition Temperatures and Enthalpies for $C_{14}H_{26}O_4$ and $C_{16}H_{30}O_4$*

Transition	T [K]		ΔH_{tot} [kcal mol^{-1}]
	$C_{14}H_{26}O_4$	$C_{16}H_{30}O_4$	
Solid–solid	397.5 ± 0.3	395.9 ± 0.3	56.9 ± 2.0[a])
Solid–liquid	398.0 ± 0.3[b])	396.4 ± 0.3[c])	60.1 ± 2.0

[a]) Lit. value: 50.2 kcal mol^{-1} [3]. [b]) Lit. value: 398.9 K [1]. [c]) Lit. value: 398.2 K [1].

1.2. *X-Ray Diffraction.* At room temperature, the X-ray powder-diffraction patterns of $C_{14}H_{26}O_4$ and $C_{16}H_{30}O_4$ were of the monoclinic $P2_1/c$ form, just as for dicarboxylic acids with a smaller number of repeating CH_2 groups ($C_{10}H_{18}O_4$, $C_{12}H_{22}O_4$) [6][23]. On heating, $C_{14}H_{26}O_4$ and $C_{16}H_{30}O_4$ adopted another $P2_1/c$ monoclinic form, 1° below their melting points. This solid–solid transition was revealed in the diffraction patterns by a slight displacement of the reflections towards higher values of 2θ, in contrast to what occurs in thermal expansion (*Fig. 2*). This behavior contrasts with that of other, shorter-chain dicarboxylic acids, where this transition does not occur, and where a thermal expansion is observed when the temperature increases [24].

Although the X-ray powder-diffraction results confirm the transition revealed by DSC, they do not conclusively identify the two polymorphs by analogy to the forms observed in the fatty acids. This is because forms *E*, *B*, and *C* observed in the unbranched fatty acids are all monoclinic ($P2_1/c$) [12][15][25–29]. The crystalline-cell parameters of the low- and high-temperature forms are reported in *Table 2*.

Table 2. *Cell Parameters for $C_{14}H_{26}O_4$ and $C_{16}H_{30}O_4$ as a Function of Temperature.* All forms are monoclinic ($P2_1/c$).

	a [Å]	b [Å]	c [Å]	β [°]	$a \sin\beta$ [Å]	Form	T [K]
$C_{14}H_{26}O_4$	15.591(2)	4.9737(2)	9.9090(6)	102.273(4)	15.235(6)	C	293
	15.549(2)	4.9682(4)	10.3300(9)	100.409(6)	15.293(8)	C_h	398
$C_{16}H_{30}O_4$	18.059(1)	4.9938(2)	9.7127(4)	105.866(2)	17.371(3)	C	293
	18.002(2)	4.9900(2)	10.1234(4)	104.056(3)	17.462(5)	C_h	396

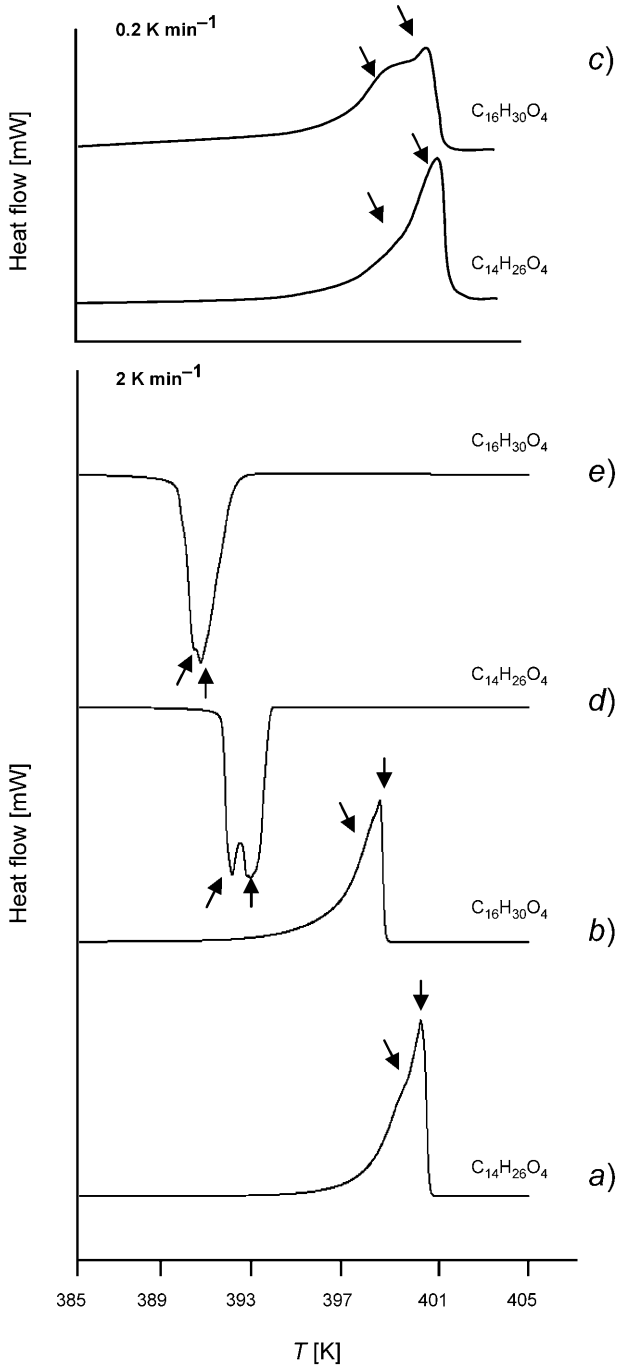

Fig. 1. *DSC Analysis for $C_{14}H_{26}O_4$ and $C_{16}H_{30}O_4$*

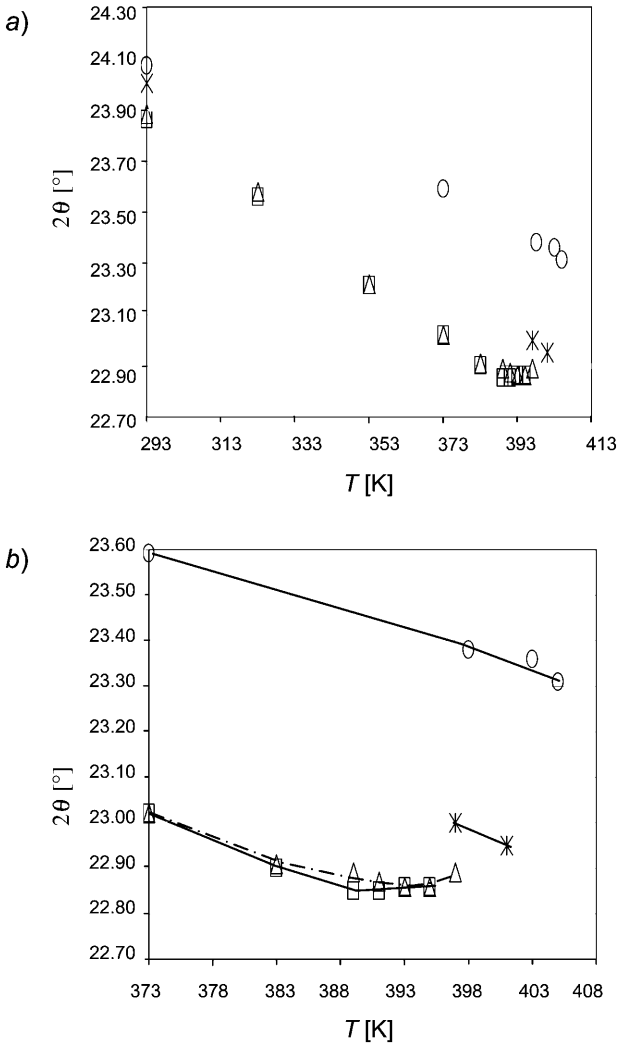

Fig. 2. a) *2θ Evolution as a Function of Temperature for the (202) reflection of Different Unbranched Diacids.* $C_{10}H_{18}O_4$ (O), $C_{12}H_{22}O_4$ (∗), $C_{14}H_{26}O_4$ (Δ), $C_{16}H_{30}O_4$ (□). b) *Zoom of* a

1.3. *IR Spectroscopy.* The IR spectra of the diacids, by analogy to the unbranched fatty acids [13][14][29], indicate that both pure compounds adopt the *C*-form at room temperature (*Fig. 3*). The $\tau(CH_2)$ band was found to split into two resonances at 730 and 720 cm^{-1} due to the O ⊥ subcell. The δ(OCO) band appeared at 688 cm^{-1}, and the signal at *ca.* 945 cm^{-1} was assigned to the σ(OH) band.

1.4. *Scanning-Electron Microscopy* (SEM) *and Thermo-Optical Microscopy* (TOM). These techniques showed regular prismatic plates for the two diacids (*Fig. 4*), with an acute angle of 54°, characteristic of the *C*-form, as observed for unbranched fatty acids [30][31]. After melting and quenching, the fatty acids metastabilize the high-

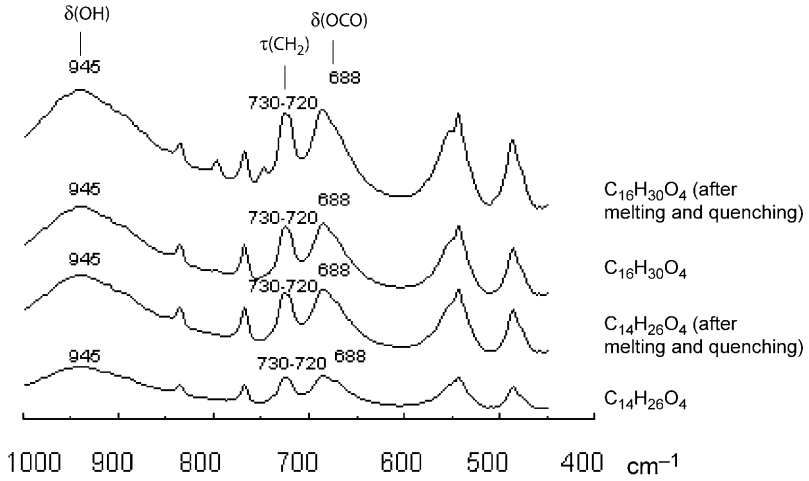

Fig. 3. *IR Spectra of* $C_{14}H_{26}O_4$ *and* $C_{16}H_{30}O_4$ *at 298 K*

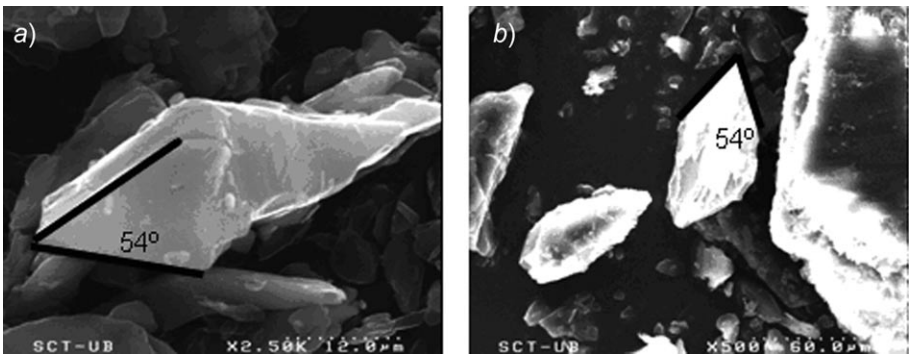

Fig. 4. *SEM Images of* a) $C_{14}H_{26}O_4$ *and* b) $C_{16}H_{30}O_4$ *at 298 K*

temperature phase at room temperature [32]. We, thus, attempted to metastabilize the high-temperature phase observed in both dicarboxylic acids by applying this process. However, the phases observed after melting and quenching the samples were the same as those of the original compounds. There were no significant differences in the crystalline-cell parameters (*Table 3*) or the IR spectra (*Fig. 3*).

Table 3. *Cell Parameters for* $C_{14}H_{26}O_4$ *and* $C_{16}H_{30}O_4$ *at 293 K After Melting and Quenching*

	a [Å]	*b* [Å]	*c* [Å]	*β* [°]	*a* sin *β* [Å]	Form
$C_{14}H_{26}O_4$	15.594(1)	4.9736(2)	9.9094(7)	102.270(5)	15.230(6)	*C*
$C_{16}H_{30}O$	18.055(1)	4.9959(1)	9.7120(3)	105.867(2)	17.375(3)	*C*

2. *Phase Diagram*. The binary phase diagram of the two diacids is shown in *Fig. 5*. It is characterized by the following parameters:

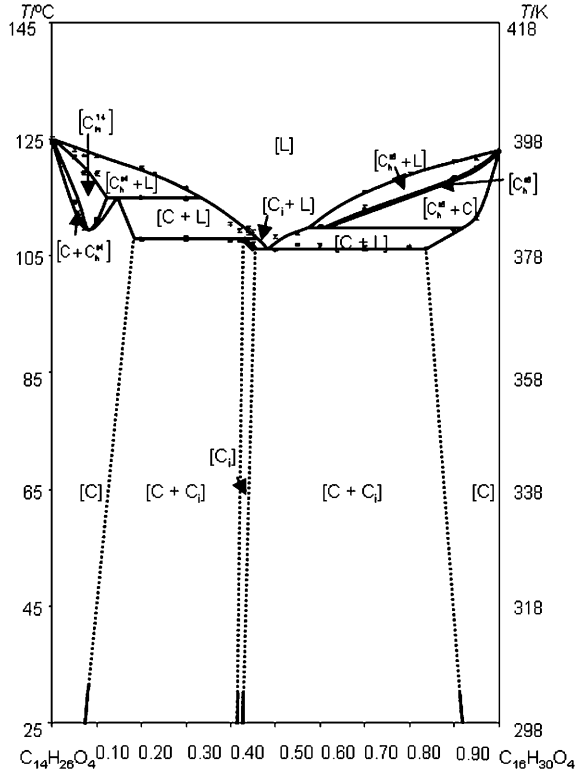

Fig. 5. *Binary phase diagram of $C_{14}H_{26}O_4$/$C_{16}H_{30}O_4$*

- Five solid–liquid domains: two $[C_h+L]$, two $[C+L]$, and one $[C_i+L]$.
- Four solid–solid domains: two $[C+C_h]$ and two $[C_i+C]$
- Five monophasic domains: two $[C]$, two $[C_h]$, and one $[C_i]$
- A minimum at *ca*. 382.7 K, with $x \approx 7$ mol-% of $C_{16}H_{30}O_4$ for the $[C+C_h]$ domain.
- Two peritectic invariants at $T_{P1} \approx 380.7$ K between $x \approx 15$ and 45 mol-% of $C_{16}H_{30}O_4$, and at $T_{P2} \approx 387.9$ K between $x \approx 10$ and 35 mol-% of $C_{16}H_{30}O_4$.
- Eutectic and metatectic invariants located at $T_{E1} \approx 379.6$ K between $x \approx 45$ and 85 mol-% of $C_{16}H_{30}O_4$, and $T_{E2} \approx 382.7$ K between $x \approx 55$ and 90 mol-% of $C_{16}H_{30}O_4$.

2.1. *Energetic Characterization*. Calorimetric measurements led to the determination of phase transitions as well as their temperatures and enthalpies. The results are listed in *Table 4*.

2.2. *Structural Characterization*. Different experiments under isothermal and isoplethic conditions were carried out for different compositions. The results allowed us to identify the various alloys, and establish the limits of their stability domains.

2.2.1. *Isothermal Analysis.* Measurements were made at 293 K. The domains $[C]$, $[C+C_i]$, $[C_i]$, $[C_i+C]$, and $[C]$ were observed when increasing the percentage of $C_{16}H_{30}O_4$. The *C*-phase was found to be the stable form of $C_{14}H_{26}O_4$ and $C_{16}H_{30}O_4$ at low temperatures, and the C_i-phase appeared as a consequence of compositional disor-

Table 4. *Transition Temperatures* (T, in K) *and Enthalpies* (ΔH, in kJ mol^{-1}) *for Binary Compositions of Tetradecanedioic and Hexadecanedioic Acid*. T_E, T_M, and T_P are eutectic, metatectic, and peritectic invariants, resp.

Mixture[a])	T_{E1}	T_{P1}	T_M	T_{P2}	$T_{solv\ inf}$	$T_{sol-sol}$	T_{sol}	T_{liq}	T_{fus}	ΔH_{fus}	ΔH_{tot}
0						397.5 ± 0.3			398.0 ± 0.3	56.9 ± 2.0	
5					387.1 ± 0.4		395.0 ± 0.4	396.3 ± 0.4			51.3 ± 1.0
7					383.1 ± 0.6		392.2 ± 0.2	395.2 ± 0.2			47.1 ± 2.0
10					384.2 ± 0.3		392.1 ± 0.5	395.0 ± 0.2			48.5 ± 1.1
20		380.8 ± 0.2		388.0 ± 0.2				393.2 ± 0.2			51.5 ± 2.0
30		381.0 ± 0.3		387.8 ± 0.2				389.7 ± 0.2			52.9 ± 1.1
40		380.6 ± 0.2						383.4 ± 0.2			49.2 ± 2.1
42		380.6 ±						382.4 ± 0.3			50.8 ±
44		382.6 ± 0.5						382.1 ± 0.5			50.7 ± 1.0
45	380.0 ± 0.4							382.0 ± 0.5			48.2 ± 1.0
50	379.0 ± 0.2							381.4 ± 0.3			47.1 ± 1.5
55	379.9 ± 0.2							381.8 ± 0.2			50.3 ± 0.8
60	379.7 ± 0.4		383.0 ± 0.2					383.0 ± 0.2			49.9 ± 1.3
70	379.4 ± 0.4						386.0 ± 0.6	389.0 ± 0.3			46.5 ± 2.2
80	379.5 ± 0.2							392.0 ± 0.2			50.3 ± 1.3
90			382.4 ± 0.4				391.3 ± 0.3	394.1 ± 0.2			50.3 ± 1.3
95					384.4 ± 0.4		393.0 ± 0.3	394.6 ± 0.3			54.7 ± 1.0
100						395.9 ± 0.2			396.4 ± 0.2	60.1 ± 2.0	

[a]) Mol-% of $C_{16}H_{30}O_4$.

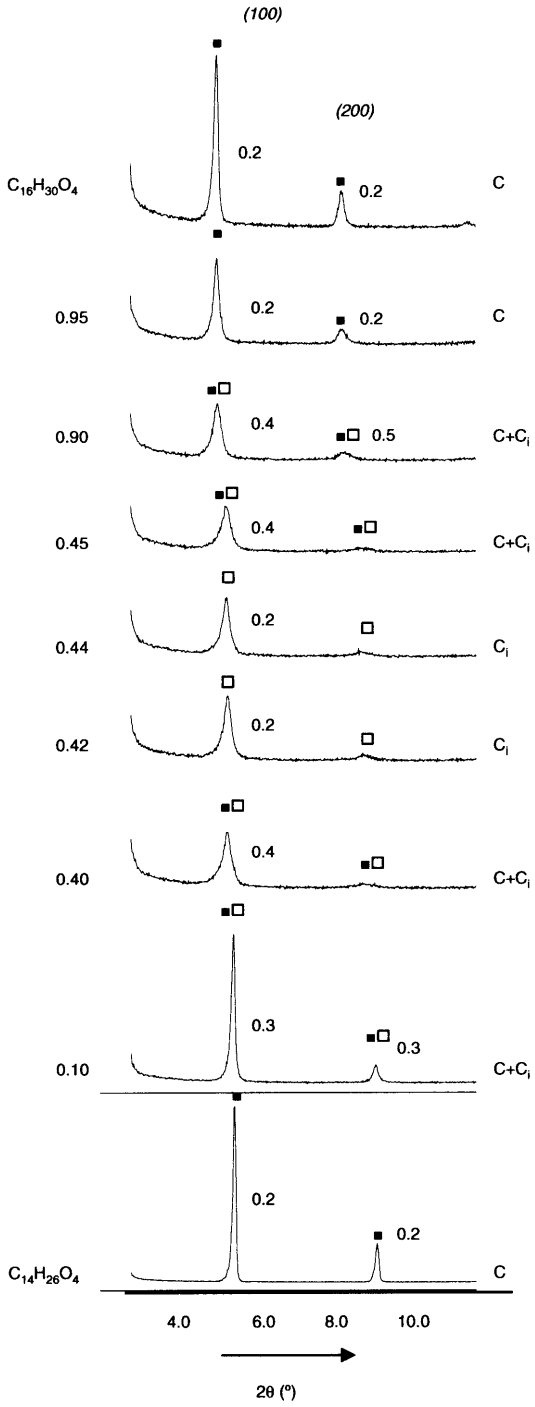

Fig. 6. *Full width at half maximum* (FWHM) *of the* (h*00) X-ray powder diffraction line as a function of binary composition. C*-Form (■), C_i-form (□).

der. These two forms belong to the same space group ($P2_1/c$), so it is difficult to differentiate between *C*- and C_i-forms. By means of powder diffraction, when *C* and C_i coexist, the full width at half maximum (FWHM) of the (*h*00) reflections increased (*Fig. 6*). No differences between *C* and C_i were observed by IR spectroscopy. The corresponding SEM and TOM images showed that all the prismatic plates had an acute angle of 54°.

2.2.2. *Isoplethic Analysis.* The isoplethic analysis of the compositions studied established the stability limits of the different phase domains as a function of temperature.

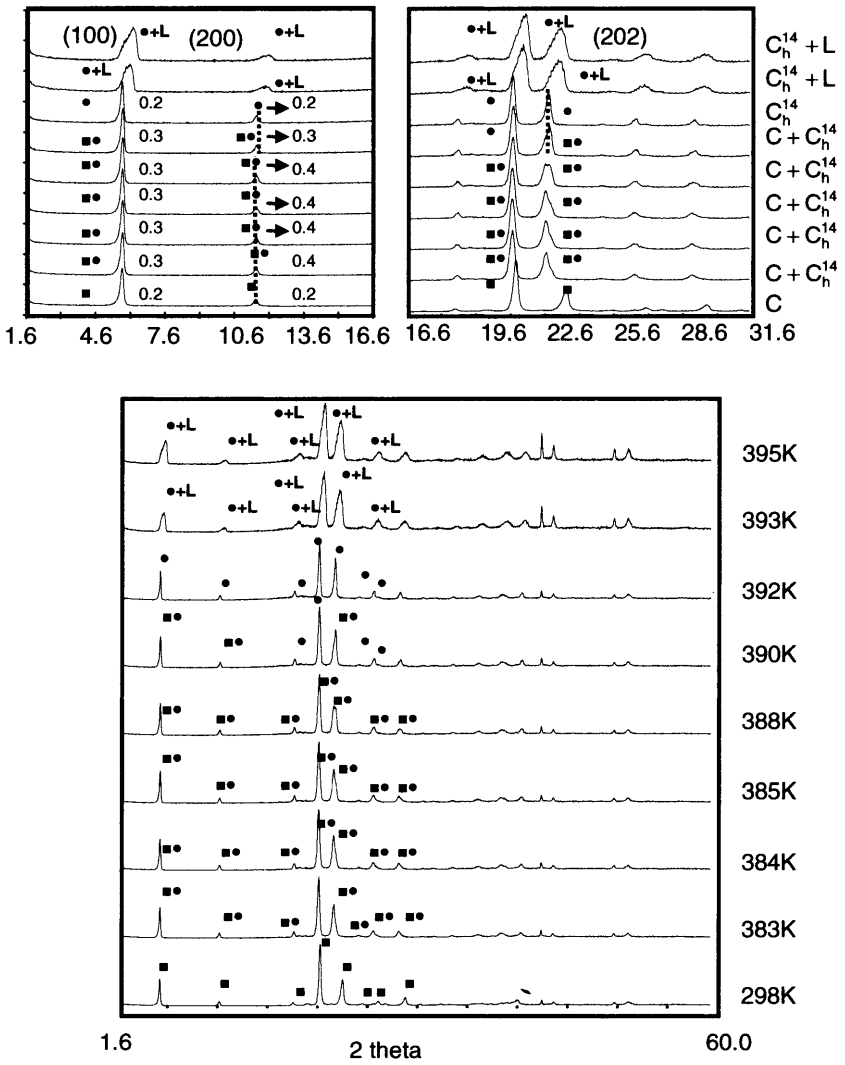

Fig. 7. *Temperature-dependent X-ray powder-diffraction diagrams for the binary mixture* $C_{14}H_{26}O_4$/$C_{16}H_{30}O_4$ *93 : 7. C*-form (■), C_h-form (●).

At a binary composition of 7 mol-% of $C_{16}H_{30}O_4$, and when the C_h-form appeared, we observed an increase in the FWHM for the (h00) reflections and a slight displacement, in contrast to what occurs under thermal expansion. Furthermore, an enfoldment was found for the (202) reflections. At higher temperatures, when the liquid appeared, an increase of the background powder-diffraction spectrum was noticed (*Fig. 7*).

Next, a binary composition of the two acids was studied for 80 mol-% of $C_{16}H_{30}O_4$. The corresponding X-ray powder-diffraction data are shown in *Fig. 8* at different temperatures. When the C_h-form appeared, the pattern was the same as that reported for the above 7 mol-% composition. The solid–liquid → solid–solid → solid–liquid transitions were corroborated by TOM. As shown in *Fig. 9*, we observed the liquid presence by a displacement of the sample spots and a round of the same. Thereby, for all com-

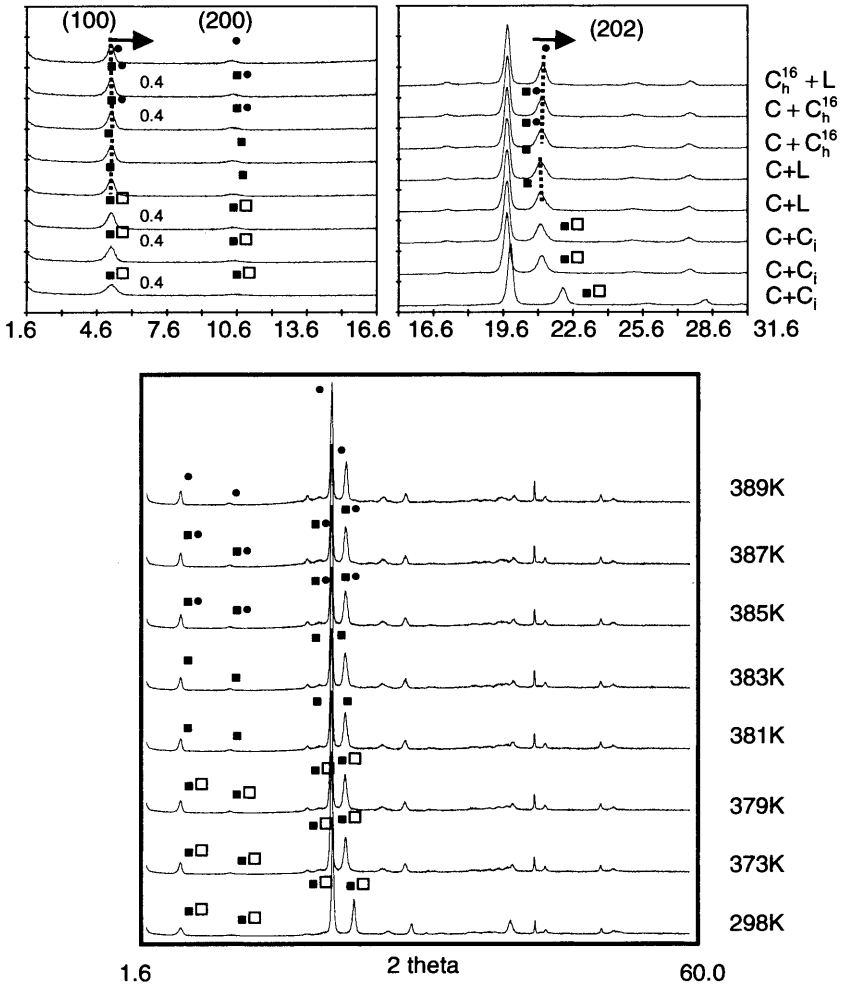

Fig. 8. *Temperature-dependent X-ray powder-diffraction diagrams for the binary mixture $C_{14}H_{26}O_4$/ $C_{16}H_{30}O_4$ 20:80. C*-form (■), C_i-form (□), C_h-form (●).

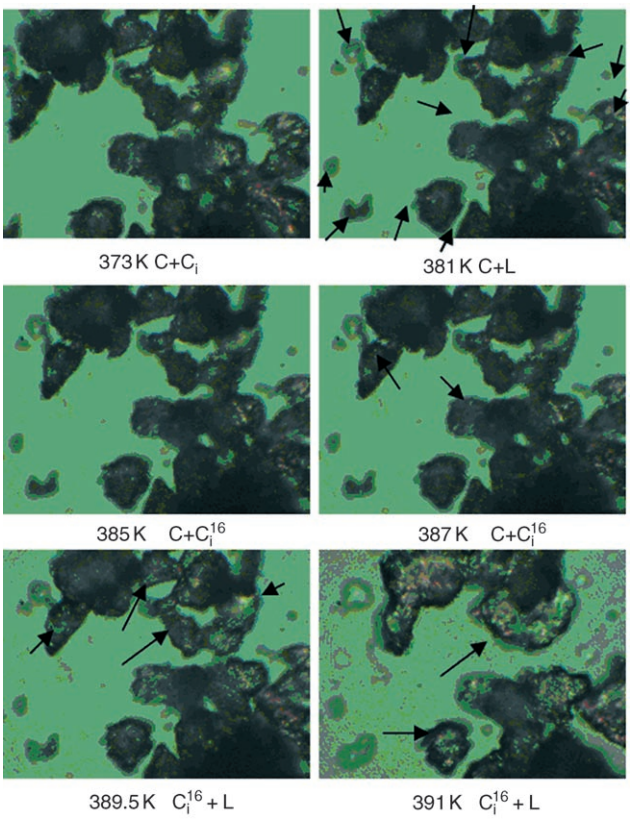

Fig. 9. *TOM Images of a the binary mixture $C_{14}H_{26}O_4/C_{16}H_{30}O_4$ 20 : 80 as a function of temperature*

positions studied, TOM measurements showed an acute angle of 54° for all the prismatic plates.

Conclusions. – Tetradecanedioic acid ($C_{14}H_{26}O_4$) and hexadecanedioic acid ($C_{16}H_{30}O_4$) display the same polymorphic behavior. The stable form at low temperature is of type *C* ($P2_1/c$). This *C*-form changes into C_h ($P2_1/c$) just below the melting point of the latter. In mixtures of the two dicarboxylic acids, a new C_i-form ($P2_1/c$) appears over a wide range of binary compositions. The similarity of the crystalline forms in the pure compounds and in the binary-phase diagram prompted us to use complementary analytical techniques to facilitate the identification and characterization of the various forms. Although both original compounds are isostructural, their phase diagram shows that there is no total miscibility: it exhibits two peritectic invariants and a minimum for compositions rich in $C_{14}H_{26}O_4$, as well as eutectic and metatectic invariants for compositions rich in $C_{16}H_{30}O_4$.

From a practical point of view, the resulting alloys cannot be considered suitable as phase-change materials (MAPCMs) for applications in the fields of thermal protection

at a controlled temperature. The difference between liquidus temperature and solidus temperature is too great.

This study was supported by *CICYT* (No. MAT2005-07965-C02-01).

REFERENCES

[1] D. M. Small, 'Handbook of Lipid Research', Plenum Press, New York, 1986.
[2] J. Housty, M. Hospital, *Acta Crystallogr., Sect. B* **1968**, *24*, 486.
[3] J. Housty, M. Hospital, *Acta Crystallogr.* **1966**, *21*, 553.
[4] N. B. Chanh, Y. Haget, J. Bèdouin, *J. Bull. Soc. Fr. Minéral. Cristalogr.* **1972**, *95*, 281.
[5] M. A. Cuevas-Diarte, Ph.D. Thesis, University of Barcelona, 1978.
[6] A. D. Bond, M. R. Edwards, W. Jones, *Acta Crystallogr., Sect. E.* **2001**, Struct. Rep. online, *57*, o141.
[7] F. Kaneko, E. Ishikawa, M. Kobayashi, M. Suzuki, *Spectrochim. Acta, A* **2004**, *60*, 9.
[8] E. von Sydow, *Acta Chem. Scand.* **1956**, *10*, 1.
[9] M. Goto, E. Asada, *Bull. Chem. Soc. Jpn.* **1978**, *51*, 70.
[10] T. R. Lomer, *Acta Crystallogr.* **1963**, *16*, 984.
[11] T. Kobayashi, M. Kobayashi, H. Tadokoro, *Mol. Cryst. Liq. Cryst.* **1984**, *104*, 193.
[12] M. Goto, E. Asada, *Bull. Chem. Soc. Jpn.* **1978**, *51*, 2456.
[13] R. F. Holland, J. R. Nielsen, *J. Mol. Spectrosc.* **1962**, *9*, 436.
[14] R. F. Holland, J. R. Nielsen, *J. Mol. Spectrosc.* **1963**, *16*, 902.
[15] F. Kaneko, M. Kobayashi, Y. Kitawgawa, Y. Matsuura, *Acta Crystallogr., Sect. C* **1990**, *46*, 1490.
[16] V. Malta, G. Celotto, R. Zanetti, A. F. Marteli, *J. Chem. Soc. B.* **1971**, 548.
[17] C. W. Bunn, *Trans. Faraday Soc.* **1939**, *35*, 482.
[18] L. Ventolà, T. Calvet, M. A. Cuevas-Diarte, M. Ramírez, H. A. J. Oonk, D. Mondieig, Ph. Negrier, *Phys. Chem. Chem. Phys.* **2004**, *6* , 1786.
[19] Y. Haget, D. Mondieig, M. A. Cuevas-Diarte, Patent FR 91/08695, EP 92915596.8, US 07/988, 949.
[20] R. Courchinoux, N. B. Chanh, Y. Haget, T. Calvet, E. Estop, M. A. Cuevas-Diarte, *J. Chim. Phys.* **1989**, *86*(3), 561.
[21] G. S Pawley, *J. Appl. Crystallogr.* **1981**, *4*, 357.
[22] Materials Studio (vers. 3.2), *Accelrys, Inc*., 2005.
[23] M. Vanier, F. Brisse, *Acta Crystallogr., Sect. B* **1982**, *38*, 643.
[24] L. Ventolà, L. Bayés, R. Benages, M. A. Cuevas-Diarte, T. Calvet, D. Mondieig, manuscript in preparation.
[25] V. Vand, W. M. Morley, T. R. Lomer, *Acta Crystallogr.* **1951**, *4*, 324.
[26] S. Abrahamsson, E. von Sydow, *Acta Crystallogr.* **1954**, *7*, 591.
[27] R. F. Holland, J. R. Nielsen, *Acta Crystallogr.* **1963**, *16*, 984.
[28] R. G. Snyder, J. H. Schachtschneider, *Spectrochim. Acta* **1963**, *19*, 85.
[29] M. Kobayashi, T. Kobayashi, Y. Cho, F. Kaneko, *Makromol. Chem. Macromol. Symp.* **1986**, *5*, 1.
[30] N. Garti, E. Wellner, S. Sarig, *Kristall und Technik* **1980**, *15*(11), 1303.
[31] K. Sato, M. Okada, *J. Crystal Growth* **1977**, *42*, 259.
[32] L. Hernquist, in 'Crystallization and Polymorphism of Fats and Fatty Acids', Eds. N. Garti, K. Sato, Marcel Dekker, New York, 1998, p. 97.

Received March 17, 2006